Type of the Paper (Article.)

Aromatic selenocyanates as a new class of non-mutagenic antimicrobial selenium compounds with pronounced activity against multidrug resistant ESKAPE bacteria

Muhammad Jawad Nasim [1], Karolina Witek [2,3], Annamária Kincses [4], Muhammad Sarfraz [1], Ewa Żesławska [5], Małgorzata Anna Marć [2], Mário Gajdács [4], Gabriella Spengler [4], Wojciech Nitek [6], Gniewomir Latacz [2], Elżbieta Karczewska [3], Katarzyna Kieć-Kononowicz [2], Claus Jacob [1,*], Jadwiga Handzlik [2,*]

[1] Bioorganic Chemistry, School of Pharmacy, University of Saarland, Campus B2.1, D-66123 Saarbruecken, Germany.

[2] Department of Technology and Biotechnology of Drugs, Faculty of Pharmacy, Jagiellonian University, Medical College, ul. Medyczna 9, 30-688 Cracow, Poland.

[3] Department of Pharmaceutical Microbiology, Faculty of Pharmacy, Jagiellonian University, Medical College, ul. Medyczna 9, 30-688 Cracow, Poland.

[4] Institute of Medical Microbiology and Immunobiology, Faculty of Medicine, University of Szeged, Dóm tér 10, H-6720 Szeged, Hungary.

[5] Department of Chemistry, Institute of Biology, Pedagogical University, Podchorążych 2, 30-084 Kraków, Poland.

[6] Faculty of Chemistry, Jagiellonian University, ul. Gronostajowa 2, 30-387, Kraków, Poland.

* Correspondence: j.handzlik@uj.edu.pl; Tel.: +48-12-620-55-84; c.jacob@mx.uni-saarland.de; Tel.: +49-681-302-3129

Abstract: Selenocyanates form an interesting class of organic selenium compounds as they serve as multifunctional agents (being the precursors of seleninic acids and diselenides in synthetic chemistry and as antimicrobial and cytotoxic agent in biology) and, due to their similarity with better known thiocyanates promise high biological activity. Yet whilst selenocyanates are common in synthetic chemistry, they are rarely considered in pharmaceutical design. Arylmethyl selenocyanates (**1-13**) have been synthesized and an insight into their structural properties using X-ray crystallography has been obtained. The compounds subsequently have been evaluated for their potential antimicrobial, nematicidal and cytotoxic activity. ADMET properties *in vitro*, using mutagenicity (AMES) and permeability (PAMPA) tests, have been determined. The compounds exhibit pronounced activity against various strains of bacteria (both Gram-positive and Gram-negative) and yeasts. Among them, benzylselenocyanate (**1**) represents the most active anti-ESKAPE agent, with potent antibacterial activity, especially against multidrug resistant MRSA strains (HEMSA 5). Our results demonstrate that the arylmethyl selenocyantes are not only non-mutagenic but also possess moderate cytotoxic activity against cancer cells.

Keywords: Reactive Selenium Species, arylmethyl selenocyanate, Cellular Thiolstat, antimicrobial, anticancer, ESKAPE, multidrug resistance.

1. Introduction

Since the discovery of the first modern antibiotics almost one hundred years ago, countless lives have been saved in the skirmish against pathogenic bacteria. Antibiotics such as the penicillin have served as important and effective weapons - and often as double-edged swords - to prevent the

onset of contagious ailments as prophylactic as well as post-infection curative agents. Since then, the quality of life (QoL) has been improving remarkably until the deadly enemy started to learn from our mistakes and instigated to develop resistance against antibiotics. Among various other reasons, overuse, misuse or extensive utilisation of antibiotics have led to the emergence of resistance in pathogenic bacteria, which has now become one of the biggest threats facing humanity [1]. The phenomenon of "resistance" to currently available antibiotics has attracted the attention of scientist for well over two decades now, and there is a considerable demand for development of antibiotics against these resistant strains of bacteria.

Nature itself is an affluent source of antibiotics [2-4]. Natural substances, acquired from medicinal as well as culinary plants like garlic and mustard, have been extensively employed as antibiotics [5-7]. These substances are usually enriched with potent phytochemicals like alkaloids, flavonoids, terpenes and polyphenols and oragnosulfur compounds [8-11]. Organosulfur compounds are widely dispersed in nature *e.g.* allicin in garlic, ergothioneine in mushrooms, thiocyanates and isothiocyanates in cruciferous vegetables [12-14]. Isothiocyanates and thiocyanates are organosulfur compounds and are well known for their potential antimicrobial and cytotoxic potential [14-17]. A remarkable upsurge in activity as well as reactivity has been observed for the selenium analogues of organosulfur compounds [18]. Although organotellurium compounds are generally more potent than sufur and selenium analogues, yet these compounds are rather toxic and unstable, therefore, not suitable for drug design [19]. Organoselenium compounds have, therefore, attracted the attention of scientists quite recently and certain compounds like ebselen have already entered the clinical trials [20].

Selenium analogues of naturally occurring thiocyanates (selenocyanates) represent an interesting class of organoselenium compounds [21]. These compounds are multifunctional in nature as they are employed as a precursor for the synthesis of various other organoselenium compounds like seleninic acids or diselenides in synthetic chemistry and as an effective cytotoxic agent in biology [22-24]. Although some organoseleno compounds have been reported as active compounds against microbes [25-27], little is known about antimicrobial activity of aromatic selenocyantes. Moreover, the literature also reveals that this class of selenocompounds has mostly been studied when attached to some "bioactive" scaffolds which may also influence their biological activity [24]. Since hardly any evidence of – chemically quite stable – benyzlselenocyanates can be found in the biological literature, we have turned our attention to this class of compounds and have focussed on the synthesis of some of the most basic arylmethyl selenocyanates (1-13, Figure 1), which indeed exhibit a rather encouraging effectiveness against a broad spectrum of biologically highly significant since antibiotic-resistant targets.

2. Results and discussion

2.1. Chemical synthesis

The arylmethyl selenocyanates (**1**-**13**) have been synthesized using appropriate commercially available arylmethyl halides (**14**-**26**) and potassium selenocyanate (Figure 1a), according to the general procedure described by Wheeler and Merriam with some modifications [28]. The compounds were obtained in satisfied yields (62-88%, see Experimental and Supplementary).

Preprints (www.preprints.org) | NOT PEER-REVIEWED | Posted: 22 February 2018 doi:10.20944/preprints201802.0142.v1

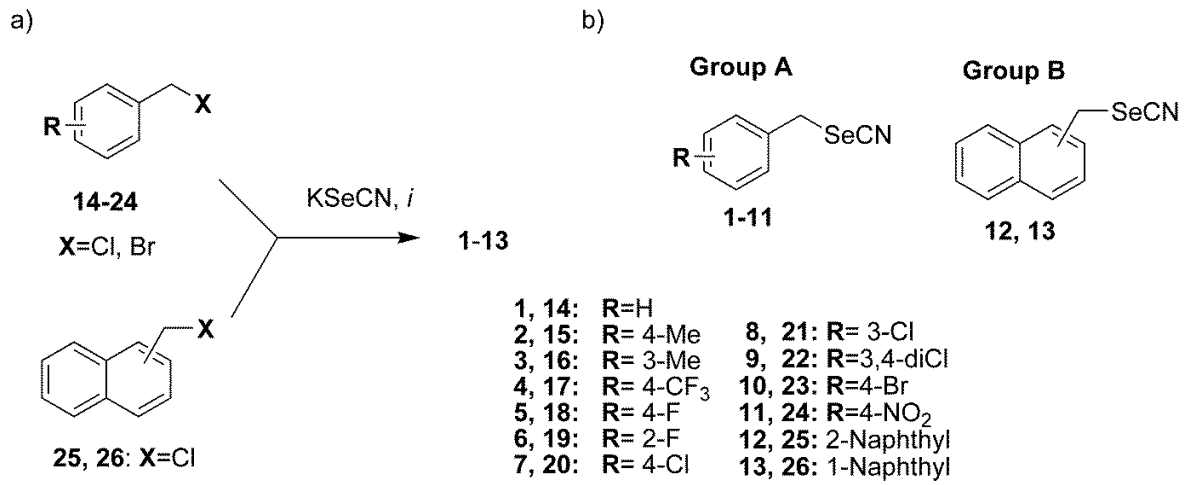

Figure 1. Synthesis (**a**) and chemical structures (**b**) of benzylmethyl (**1**-**11**, group A) and naphthylmethyl (**12**, **13**, group B) selenocyanates; *i:* ethanol, reflux, 6h.

2.2. Crystallographic studies

The structures of compounds **1**-**13** were confirmed by ^{1}H and ^{13}C-NMR and the molecular masses as well purity were confirmed by LC-MS. Additionally, a deeper insight into the structures of two selected compounds (**1** and **12**) was stipulated by employing X-ray crystallographic analysis (Table 1, Figure 2 and Figure 3).

The molecular structures and atomic-numbering schemes of **1** and **12** are presented in Figure 2. In both crystal structures the unit cells consist of four molecules. The values of bond lengths formed by the selenium atom for C(sp)-Se are 1.850 Å and 1.837 Å for compound **1** and **12**, respectively, whereas for C(sp3)-Se the bond length is 1.991 Å for both structures. Similar values were observed in other crystal structures with selenium atom [29,30]. The geometries of the methyleneselenocyanate groups in both compounds differ slightly. The responsible angles have values C1-Se1-C2 = 95.2° and 95.5°, Se1-C2-C3 = 113.7° and 114.3°, C1-Se1-C2-C3 = -62.4° and -66.5°, Se1-C2-C3-C4 = 98.6° and 98.8°, whereas the torsion angle N1-C1-Se1-C2 exhibits a significant difference of -164.4° and 67.3° for compound **1** and **12**, respectively. Methylselenocyanate fragments were also searched in the Cambridge Structural Database (CSD, Version 5.37) [31], which resulted in five crystal structures (in one case two independent molecules). In these crystal structures the values of torsion angle N1-C1-Se1-C2 were 66.8°, -170.9°, -139.5°, 29.4°, -131.7° and -173.1°. The search of the CSD demonstrated that the geometry of the methyleneselenocyanate moiety in **1** and **12** is not exceptional among structures containing this fragment. The crystal structure of **1** has been determined earlier but without hydrogen atoms [30].

(a)

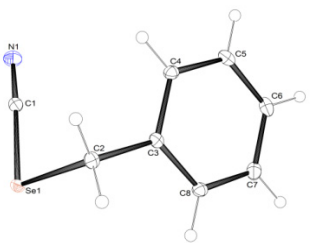

Preprints (www.preprints.org) | NOT PEER-REVIEWED | Posted: 22 February 2018 doi:10.20944/preprints201802.0142.v1

(b)

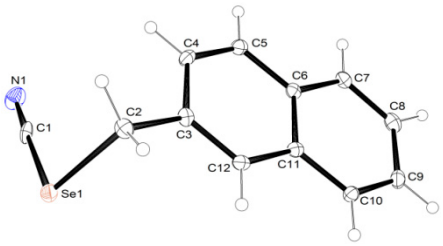

Figure 2. The molecular structure of (**a**) **1** and (**b**) **12**, with the appropriate atomic- numbering scheme. Displacement ellipsoids are drawn at 30% probability level.

The packing of the molecules in the crystal structures can be characterized by intermolecular interactions listed in Table 1. In both structures, only weak C-H···N contacts with another arrangement of molecules are observed (Figure 3).

Table 1. Parameters of intermolecular C-H···N interactions for **1** and **12**

Compounds	D-H···A	H···A [Å]	D···A [Å]	D-H···A [°]	Symmetry codes
1	C2-H2A···N1	2.59	3.559(3)	174	-x, -y, -z
	C2-H2B···N1	2.73	3.328(3)	119	x+1, y, z
	C6-H6···N1	2.84	3.513(3)	128	-x, y-1/2, -z+1/2
12	C2-H2A···N1	2.58	3.487(2)	155	x+1/2, -y+1, -z
	C2-H2B···N1	2.76	3.333(1)	118	x, y-1, z
	C8-H8···N1	2.75	3.520(2)	141	x-1/2, y-1/2, z-1/2

(a)

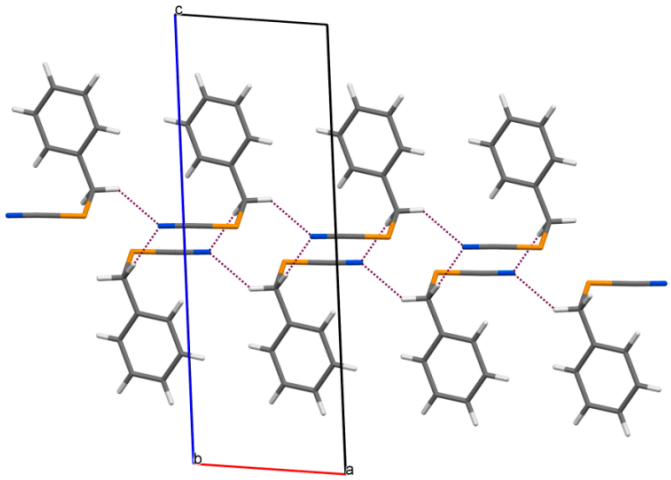

(b)

Preprints (www.preprints.org) | NOT PEER-REVIEWED | Posted: 22 February 2018 doi:10.20944/preprints201802.0142.v1

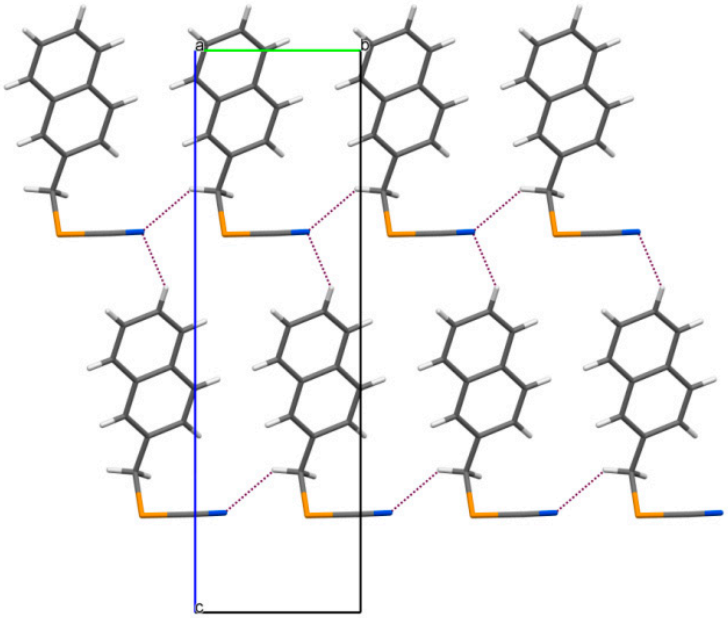

Figure 3. Partial packing views, indicating the intermolecular interactions in a layer of (**a**) selenocyanate **1** and (**b**) selenoyanate **12**. The intermolecular interactions are depicted as dashed lines.

2.3. Antimicrobial activity

Compounds **1**-**13** were initially assessed for their potential antimicrobial activity against selected bacteria (both Gram-positive and Gram-negative), fungi, and multicellular nematodes. Minimum inhibitory concentration (MIC) values have been determined against bacteria and fungi and have been compared to the reference antimicrobial agents (Table 2) [26,32-36]. Most of the compounds displayed significant antimicrobial activity against both Gram-positive and Gram-negative members of dangerous ESKAPE family [27]. In the case of Gram-positive bacteria, the compounds have been examined against the reference strain (ATCC 25923) and the multidrug resistant (MDR) clinical isolate of *S. aureus* (HEMSA 5). It is noticeable that all compounds, except **11**, displayed MIC values much lower than that of reference oxacillin against the MDR strain [26,32]. In the case of the most active compound (**1**), an excellent antimicrobial action was observed against HEMSA 5 which falls into the range of oxacillin against the susceptible strain ATCC 25923 (Table 2). Moreover, seven compounds (**2**, **3**, **6**, **8**, **9**, **12** and **13**) demonstrated anti-staphylococcal activity with MIC values lower than 10 μg/ml. Interestingly, the series of compounds did not discriminate between referent and MDR *S. aureus* strains and displayed similar antibacterial potency against both or even slightly stronger against the MDR strain (**12**). This indicates the ability of the selenocyanates to overcome bacterial MDR, most likely by by-passing the components responsible for resistance, which is of great significance when searching for new therapeutic solutions in the face of a significant drop in antibiotic effectiveness today.

Table 2. Antimicrobial activity of arylmethyl selenocyanates (**1**-**13**)

Cpd	MICs (μg/ml)						
	S. carnosus	*S. aureus* ATCC25923	MRSA* HEMSA 5	*A. baumannii* 4184/2/5	*P. aeruginosa* *4600*	*C. albicans*	*S. cerevisiae*
1	24.48	**≤ 0.76**	**0.76**	**1.53**	**6.12**	**12.24**	24.48
2	26.27	**6.57**	**6.57**	**6.57**-13.14	52.54	52.54	52.54
3	**13.19**	**6.59**	**6.59**	**13.19**	26.37	**13.19**	**6.59**
4	264.08	**16.51**	33.02	33.01	33.01	264.08	66.04
5	53.52	≥ 26.76	>26.76	26.76	26.76	**6.69**	53.52
6	**6.69**	**6.69**	**6.69**	**13.38**	107.05- 210.10	**6.69**	**6.69**
7	230.4	**14.8**-28.8	28.8	14.4-28.8	28.8	**7.4**	460.8
8	115.28	**7.2 –** 14.4	**7.2 -** 14.4	**7.2** – 14.4	115.28	28.82	28.82
9	33.13	**8.28**	**8.28**	**8.28 –** 16.56	66.25	33.13	66.25
10	275.04	34.38	>34.38	34.38	34.38	275.04	68.76
11	30.125	482	482	>482	>482	**7.53**	60.25
12	123.09	**15.44**	**7.72**	**15.44**	246.17	61.55	123.09
13	**15.39**	**7.69**	**7.69**	**15.39**	246.16	30.78	61.56
Ref.	0.03[a]	0.45[b]	128[b]	<4[b]	≤16 [c]	0.094-4[d]	0.03-2[e]

*MRSA; methicillin-resistant *S. aureus*; MIC values for reference antibiotics: [a]ampicillin, [b]oxacillin, [c]piperacillin [d]fluconazole and [e]itraconazole [27,32-36].

As for Gram-negative bacteria, compound **1** demonstrated excellent antimicrobial activity, especially against pathogenic *A. baumannii* and *P. aeruginosa*. In these cases, compound **1** was more potent than the reference drugs, *i.e.* oxacillin and piperacillin [33,34]. Interestingly, a significant decrease of antibacterial activity of **1** was observed in the case of non-pathogenic *S. carnosus* which highlights the selective targeting of this compound towards pathogenic bacteria. Compounds **2, 3, 6, 9, 12** and **13** also demonstrated a pronounced activity against *A. baumannii* (MIC< 20 μg/ml).

In the context of pathogenic yeasts, compounds **1**, **3**, **5**, **7** and **11** displayed activity against *C. albicans* and inhibited the growth at concentrations even below 20 μg/ml. The highest activity, almost in the range of clinically relevant antifungal drugs [35,36], has been observed for compounds **5**, **7** and **11** with MIC < 10 μg/ml (Table 2). The apparent activity of these compounds against *C. albicans* suggests their possible application as potent antifungal agents. The aromatic selenocyanates, however, have not exhibited a significant activity against non-pathogenic *S. cerevisiae*. Here, just compound **3** inhibited the growth at the concentration below 20 μg/ml (*i.e.* at 6.59 μg/ml), yet its activity against this pathogenic fungus was distinctly lower than that of the benchmark fungicide itraconazole [35,36].

2.4. Nematicidal activity

In order to extend the scope of preliminary studies focused on unicellular organisms, such as bacteria and yeasts, another assay involving multicellular organisms of parasites has been employed. Thus, the whole series (**1**-**13**) has been evaluated for nematicidal potential against the agricultural nematode *S. feltiae,* which represents a simple and reliable multicellular model system (Figure 4).

Preprints (www.preprints.org) | NOT PEER-REVIEWED | Posted: 22 February 2018 doi:10.20944/preprints201802.0142.v1

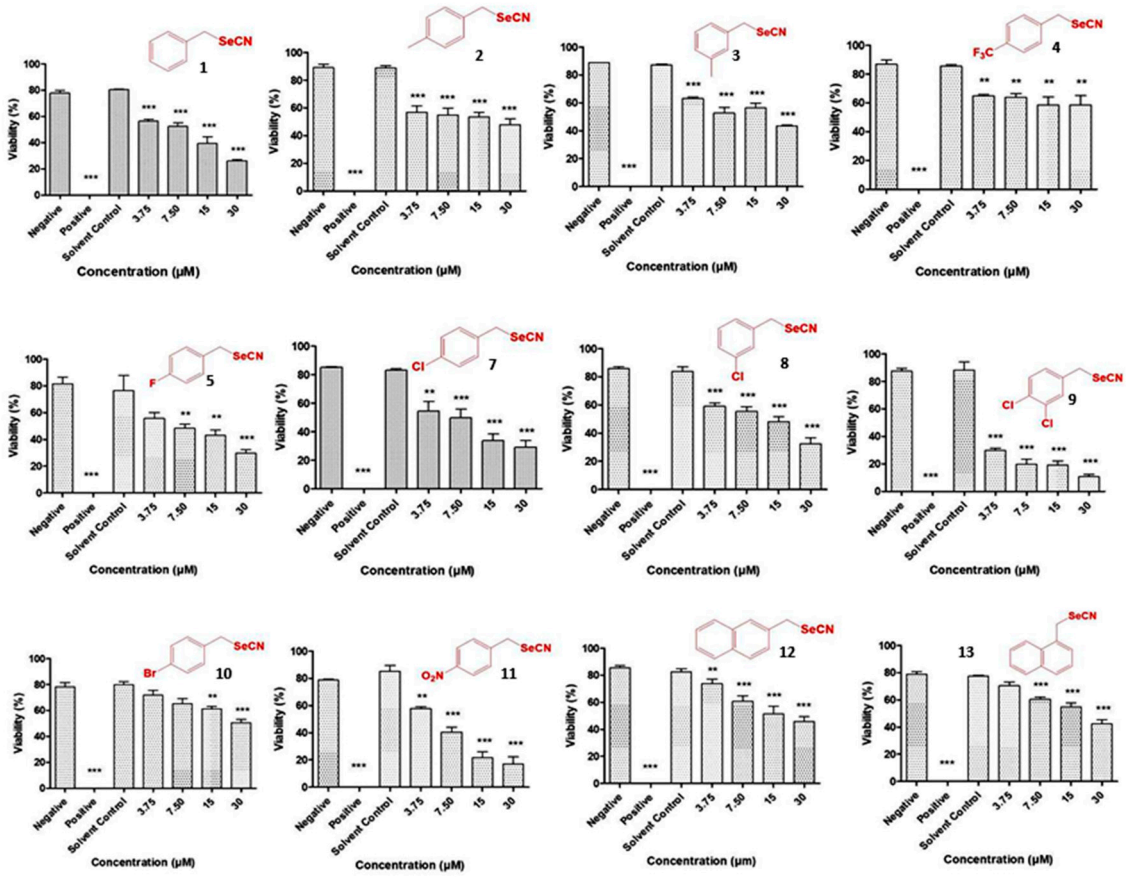

Figure 4. Concentration-dependent activity of selenocyanates against *S. feltiae*. Ethanol (70% v/v) was used as positive control and PBS buffer was used as negative control. Values represent mean ± S.D. *** $p < 0.001$ and ** $p < 0.01$.

Compounds have been evaluated at the concentrations ranging from 3.75 μM to 30 μM and all of them caused a remarkable, concentration-dependent decrease in the viability, which was pronounced even at the lowest concentrations tested. As for the Gram-negative bacteria compound **1** stands out as it exhibited either similar or even higher nematicidal activity as compared to other compounds, with the exception of compounds **9** and **11**. Although agricultural applications are more speculative at this time, these results indicate that the selenocyanates may also serve as excellent nematicidal agents, possibly also against pathogenic nematodes affecting animals and humans.

2.5. Influence of arylmethyl selenocyantes on mammalian cells

In order to investigate any selectivity for microorganisms and to rule out any major cytotoxicity against mammalian cells, compounds **1**-**12**were investigated for their possible cytotoxicity against the normal NIH/3T3 mouse embryonic fibroblast cell line and two cancer cell lines of mouse T-lymphoma, *i.e.* the sensitive (PAR) and the multidrug resistant cell line (MDR) transfected with the human *MDR1 (ABCB1)* gene that codes for the ABC transporter. Doxorubicin was used as positive control (Table 3). Furthermore, the efflux pump inhibitory activity of selected compounds (**1**, **2**, **4**, **5**, **7** and **11**) was investigated in both cancer cell lines (PAR and MDR) using the rhodamine 123 accumulation assay, that allowed to evaluate rhodamine 123 (R123) retention by flow cytometry. Verapamil was employed as reference inhibitor (Table 4) [37,38].

Preprints (www.preprints.org) | NOT PEER-REVIEWED | Posted: 22 February 2018 doi:10.20944/preprints201802.0142.v1

2.5.1. Cytotoxicity in cancerous and non-cancerous cell lines

According to the results (Table 3), none of the compounds exhibited any significant inhibitory activity against the non-cancerous NIH/3T3 mouse fibroblast cells. In both T-lymphoma cell lines, compounds **4**, **5**, **7** and **10** were considerably less cytotoxic when compared to the reference doxorubicin. Intriguingly, compounds **1-3, 6, 8, 9, 11** and **12** displayed significant cytotoxic effects on the parental and multidrug-resistant sublines of mouse T-lymphoma cells.

Table 3. Cytotoxic effects of arylmethyl selenocyanates on both, non-cancerous and cancer cells.

Cytotoxic effects on non-cancerous and cancer cells							
Cpd	**Non-cancerous**		**Mouse T-lymphoma cells**				**SI**
	NIH/3T3		**PAR**		**MDR**		
	IC_{50} (μM)	**SD ±**	**IC_{50} (μM)**	**SD ±**	**IC_{50} (μM)**	**SD ±**	
1	31.00	3.24	5.84	0.45	7.69	0.66	0.76
2	55.12	2.81	5.33	0.41	9.72	1.1	0.55
3	29.58	0.95	9.03	0	5.95	0.18	1.52
4	>100	-	89.18	2.33	>100	-	≤0.89
5	>100	-	>100	-	>100	-	ND
6	59.94	0.35	7.93	0.36	8.08	0.75	0.98
7	>100	-	>100	-	>100	-	ND
8	44.73	1.79	8.58	0.18	9.64	0.88	0.89
9	42.17	3.08	8.53	0.39	10.32	1.13	0.83
10	>100	-	>100	-	>100	-	ND
11	70.08	1.55	7.26	0.74	14.09	1.58	0.52
12	24.18	1.97	8.47	0.1	7.05	0.15	1.20
DOX	13.38	0.98	0.42	0.17	2.64	0.09	0.16
DMSO	>2 V/V%	-	>2 V/V%	-	>2 V/V%	-	ND

NIH/3T3, non-cancerous mouse embryonic fibroblast cells; PAR, parental T-Lymphoma cells; MDR, multidrug resistant T-Lymphoma cells overproducing efflux pump Pgp; DOX, doxorubicin; DMSO, dimethyl sulfoxide; SD, standard deviation; SI, selectivity index; ND, not determined.

Although the compounds investigated (**1**-**12**) did not exhibit any distinct selectivity, the substantial activity of compounds **1**, **3** and **12** against MDR cells is worth noticing. Thus, aromatic selenocyanates **1**-**3**, **6**, **8**, **9**, **11** and **12** may not only be of interest in the context of antimicrobial action - as anticipated initially - but also as a starting point in further search for anticancer agents with MDR-reversing properties.

2.5.2. Cancer MDR efflux pump inhibitory properties

As some of the selenocyanates demonstrated cytotoxic activity against MDR subline of mouse T-lymphoma cells, the compounds were evaluated for their potential as the inhibitors of efflux pump. None of the compounds exhibited significant ABCB1 inhibitory activity as compared to the positive control (verapamil, 20 μM) on the cell line under investigation (Table 4). Nonetheless compound **11** demonstrated 49.29% inhibition (FAR = 5.62) at higher concentration (20 μM) whilst compounds **1** and **2** exhibited only 16.05% and 17.28% inhibition respectively *i.e.* around 3-times

Preprints (www.preprints.org) | NOT PEER-REVIEWED | Posted: 22 February 2018 doi:10.20944/preprints201802.0142.v1

lower than that of the **11**. None of the compounds, however, demonstrated any significant inhibitory activity (ranging between 5.52-11.75%) at lower concentration (2 μM) when compared to positive control (verapamil) and previously evaluated selenoesters and selenoanhydride [38].

Table 4. Effects of selenocyanates on rhodamine 123 accumulation by multidrug resistant (MDR) mouse T-lymphoma cells.

Cpd	Effects on rhodamine 123 accumulation			
	Concentration 2 μM		Concentration 20 μM	
	FAR	FAR quotient (%)	FAR	FAR quotient (%)
1	0.82	7.19	1.83	16.05
2	0.978	8.58	1.97	17.28
4	0.76	6.67	0.61	5.35
5	0.82	7.19	0.82	7.19
7	0.927	8.13	0.731	6.41
11	0.63	5.52	5.62	49.29
13	1.34	11.75	0.72	6.32
VER	-	-	11.4	100.00
DMSO	0.63 (V/V%)	5.52	-	-

VER, verapamil; FAR, fluorescence activity ratio; FAR quotient: FAR of a compound related to FAR of VER tested at 20 μM.

2.6. ADMET studies in vitro

Since the series of selenocyanates under investigation demonstrated pronounced antimicrobial and nematicidal activities, it was important to investigate their "drug-likeness" profile. Four compounds (**1**, **2**, **4** and **13**) were selected for the *in vitro* assays on safety and absorption properties. The mutagenic potential of compounds was evaluated employing modified Ames fluctuation test [27,39,40], and membrane permeability was estimated using the Parallel Artificial Membrane Permeability Assay (PAMPA) (Figure 5, Table 5) [40-42].

2.6.1. Mutagenicity

The Ames fluctuation experiments were performed in triplicate to provide a mutagenic index (MI), computed according to the method described previously (Table 5) [27]. Binomial B-values were calculated according to the manufacturer's instructions (Xenometrix AG, Allschwil, Switzerland). Compounds under investigation were considered mutagenic if MI > 2.0 and B ≥ 0.99 [27,39,40].

Results of the experiments indicate very clearly that neither the selenocyanates (**1, 2, 4, 13**) nor the reference ebselen displayed any mutagenic potential at a concentration of 1 μM. Compounds **1, 2** and **13** were also non-mutagenic at the higher concentration of 10 μM. Solely compound **4,** at the higher concentration (10 μM), exhibited an increased Binomial B – value (B = 1.0), which may point towards a probable mutagenic potential. The mutagenicity of this derivative is rather ambiguous, as the value of the second parameter indicative of mutagenicity (MI = 1.75) was still below the threshold of 2.0, and substantially lower than the MI value for the mutagenic reference NQNO with a MI = 6.91 calculated at a concentration of 0.5 μM (Figure 5, Table 5).

Preprints (www.preprints.org) | NOT PEER-REVIEWED | Posted: 22 February 2018 doi:10.20944/preprints201802.0142.v1

2.5. *In vitro PAMPA permeability*

The PAMPA permeability screening test imitates the structural and biological conditions of the cell membrane and allows for a quick and simple determination of a given compound's passive transport through biological membranes, characterized by a permeability coefficient (Pe). A pre-coated PAMPA Plate System Gentest™ (Corning, Tewksbury, MA, USA) was employed, which guarantees good predictability and correlation of data obtained for human absorption in the Caco-2 cell line. The concentrations of the compounds tested in the donor and acceptor compartments were estimated by the capillary electrophoresis method (CE) as described previously [40-42]. The permeability results obtained were compared with the data for the reference drugs, *i.e.* high permeable caffeine and low permeable norfloxacin (Table 5). All compounds (**1**, **2**, **4** and **13)** exhibited good permeability with Pe values above the threshold for highly permeable compounds (>1.5 × 10^{-6} cm/s) [42]. The results calculated for compound **13** may, however, be ambiguous due to the instability of the compound in phosphate buffered saline (pH 7.4), as around 50 % decomposition was determined by controlled LC/MS analysis (data not shown).

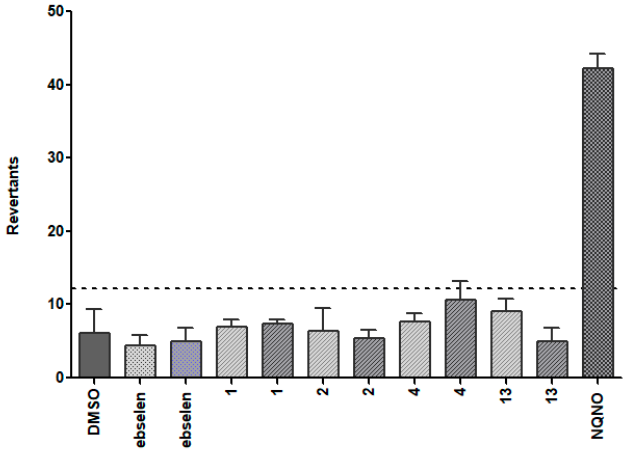

Figure 5. Results of the Ames liquid microtiter test indicative of mutagenic potential; DMSO (1% in growth medium)- negative control, ebselen (reference compound) at the concentration 1μM and 10 μM, NQNO (4-nitroquinoline-*N*-oxide, benchmark mutagenic agent) at concentration 0.5 μM; **1**, **2**, **4** and **13** - selenocyanates at concentrations 1 μM and 10 μM, ----- baseline defining the mutagenicity threshold (significant mutagenicity above this line).

Table 5. ADMET properties for some of the most active antibacterial agents (**1**, **2**, **4**, **13**).

ADME – Tox properties					
	Mutagenic potential				PAMPA - permeability
Cpd	**MI (1 μM)**	**B**	**MI (10 μM)**	**B**	**Pe [cm/s]**
1	1.15	0.74	1.20	0.81	2.69 x10^{-6}
2	1.04	0.56	0.87	0.28	3.17 x10^{-6}
4	1.25	0.87	1.75	1.0	2.57 x10^{-6}
13	1.47	0.96	0.82	0.14	2.25 x10^{-6}
Ebselen	0.69	0.26	0.80	0.46	nd
Caffeine	nd	nd	nd	nd	3.61 x10^{-6}

 doi:10.20944/preprints201802.0142.v1

Norfloxacin	nd	nd	nd	nd	0.95 x10^{-6}

Ebselen – reference compound in Ames test. Reference compounds in PAMPA: high-permeable drug, caffeine; low-permeable drug, norfloxacin. MI – mutagenic index (the quotient of the number of revertant colonies induced in a test sample and the number of revertants in a negative control). B - Binomial B value, nd – not determined; Pe - permeability coefficient.

2.8. SAR-discussion

Although a variety of the biological activities seemingly associated with compounds **1**-**13** is, undeniably, associated with the reactive selenocyanate motif, the size and substituents of the aromatic fragments seem to present significant factors that affect both, the direction as well as strength of the identified activities, and for this reason also selectivity.

The SAR analysis indicates that the unsubstituted benzyl was evidently the most favourable aromatic fragment (compound **1),** responsible for the highest antibacterial properties against all ESKAPE pathogens involved in this study, with special accent on an excellent potency against the MDR *S. aureus* (HEMSA 5), placing compound **1** in the range of the best antimicrobial drugs. In comparison to the rest of compounds investigated (**2**-**13**), the benzylselenocyanate (**1**) also demonstrated remarkable antifungal as well as nematicidal properties. Compound **1** also exhibited the strongest cytotoxic action on both, parental and multidrug resistant T-lymphoma cells.

Apart from the unsubstituted benzyl derivative (**1**), significant anti-staphylococcal activity was also observed for compounds containing the benzyl ring substituted with methyl (**2**, **3**), fluorine (**6**) and chlorine (**8**, **9**), predominantly at *meta* and/or *para* position. Moreover, both 1- and 2-naphthylmethyl derivatives (**12** and **13**, respectively) exhibited noteworthy antibacterial activities against *S. aureus* and *A. baumanni*.

Untypically, the *β*-naphthyl derivative (**12**) was more active against the MDR strain (HEMSA 5) at the lower concentration as compared to the non-resistant reference strain (ATCC 25923). The comparable MICs of benzyl and naphthyl derivatives against both *S. aureus* strains, or even lower for the MDR one, indicate not only antibacterial but also distinct reversal-MDR mechanisms of action for these Reactive Selenium Species. Although the MDR mechanism of HEMSA 5 is rather complex and has not been thoroughly explored until now, a predominant contribution of protein efflux pumps is highly probable. The potent and most effective bacterial efflux pump inhibitors (EPIs), *e.g.* peptidomimmetics or naphthylmethylpiperazine (NMP) [43] contain benzyl and/or naphthyl moieties in their chemical structures. This strongly supports the notion that the interesting antibacterial activities, observed for compounds **1**, **12** and **13,** were conditioned by the reactive SeCN-fragment on one hand, and by the unsubstituted benzyl or naphthyl moieties which are likely to inhibit the MDR efflux mechanisms, on the other. Interestingly, the 1-naphthyl derivative (**13**) also exhibited some toxicity against non-pathogenic *S. carnosus*, whilst the 3-methylbenzyl (**3**), was active against all bacteria and yeast at the concentration below 30 μM.

In the case of antifungal activity against *C. albicans*, the role of the substituent position at the benzene ring seems to play a crucial role. Thus, the three most active agents were *para*-substituted with fluorine (**5**), chlorine (**7**) and NO_2 (**11**), respectively. Interestingly, the *p*-nitrobenzylselenocyanate (**11**) exhibited the most selective activity against *C. albicans* compared to the rest of the microbes tested, yet was not active against agricultural pest nematodes. Although the strongest nematicidal effect was observed for 3,4-dichlorobenzyl compound (**9**), the second most

 doi:10.20944/preprints201802.0142.v1

active compound was the 4-nitrobenzyl derivative (**11**), which was one of the three most active cytotoxic agents effective against both, parental and multidrug resistant mouse T-lymphoma cells.

Generally, elemental selenium as well as simple organic selenium compounds interact with the cellular thiolstat and modulate the redox state of cancer cells [44]. Several simple organoselenium compounds, such as aromatic selenoesters and anhydrides exhibit excellent cytotoxicity [45] and Pgp-inhibitory activities in the corresponding assays [38,46]. The combination of the selenocyanate functional group with arylmethyl moiety, however, does not seem to be effective for cytotoxic or MDR-reversing activity in cancer cells. For cytotoxicity SAR, the methyl (**2** and **3**) and the unsubstituted benzyl (**1**) and *β*-naphthyl (**12**) fragments exhibited the highest cytotoxic activity against T-lymphoma cell lines, with a slight discrimination between parental and MDR cells. The cancer MDR inhibitory activities were almost negligible for the selenocyanates tested, with an exception of the 4-nitrobenzyl selenocyante (**11**), which demonstrated moderate activity *i.e.* 2-fold lower than that of verapamil.

Similar selenocompounds (incuding benzoselenophene-diones and various selenoesters) have also been evaluated in murine lymphoma and human adenocarcinoma cell lines overexpressing the ABCB1 transporter [38]. The cyclic selenoanhydride and the various selenoesters were several times more potent than verapamil, but the nature of their substituents at the aromatic ring seemed to influence the SAR properties to a lesser extent. In the case of the selenocyanates, the modification of the substituents in the *para*-position significantly influenced the efflux pump inhibitory properties. The strong electron-withdrawing NO_2 group has been observed to play a promoting role. The methylselenocyante substituent at an aromatic ring, presumably due to some bio-isosteric analogy with the carboxylic moiety, seems to be a main factor responsible for a considerable decrease in the ABCB1 modulatory properties of all aromatic selenocyanates (**1**-**13**) as compared to previously investigated selenoesters [38,46].

3. Conclusions

The comprehensive studies presented in the previous sections, have provided new insight into the chemistry and biological activity of small aromatic selenocyanates, which may be useful in the hunt for new antimicrobial and anticancer agents. An overview on the full spectrum of biological screening results allows to perceive a general trend for the arylmethyl selenocyanates (**1**-**13**) that comprises of the pronounced antimicrobial and antiparasitic properties with moderate cytotoxic and weak efflux pump inhibitory properties in cancer cells as well as a lower toxic activity against non-pathogenic organisms and cell lines. SAR studies indicate that benzylselenocyanate (**1**) can be selected as the best lead structure, distinctly the most active one during these studies. Indeed, compound **1** not only showed an excellent activity against multidrug resistant *S. aureus*, but also a significant action against Gram-negative pathogens, pathogenic yeasts, parasites and cancer T-lymphoma growth. Our initial ADMET screening *in vitro* has also confirmed the lack of mutagenic effects and a good permeability for compound **1**. Noteworthy, antibacterial properties were also observed for naphthyl derivatives (**12**, **13**), and antifungal for 4-fluorobenzylselenocyanate (**5**). Additionally, methylbenzyl (**2** and **3**) and *β*-naphthyl derivatives (**12**) have been identified as more attractive lead structures in the ongoing search for anticancer agents.

Since the arylmethyl selenocyanates have demonstrated considerable activity against both, pathogenic bacteria and a yeast, and were also rather potent against the problematic MDR

 doi:10.20944/preprints201802.0142.v1

345 microorganisms, future studies in the field of antimicrobial agents should consider these simple
346 structures as part of innovative drug design.

347 4. Experimental section

348 *4.1. Chemical synthesis*

349 ^{1}H NMR and ^{13}C NMR spectra were recorded on a Varian Mercury-VX 300 MHz PFG
350 instrument in DMSO-d6 at ambient temperature using the solvent signal as an internal standard.
351 The values of the chemical shifts are expressed in δ values and the coupling constants (*J*) in Hz. Mass
352 spectra were recorded on a UPLC–MS/MS system consisted of a Waters ACQUITY® UPLC®
353 (Waters Corporation, Milford, MA, USA) coupled to a Waters TQD mass spectrometer (electrospray
354 ionization mode ESI-tandem quadrupole). The UPLC/MS purity of all the final compounds was
355 confirmed to be higher than 95%. Retention times (t_R) are given in min. Thin-layer chromatography
356 was performed on pre-coated Merck silica gel 60 F254 aluminium sheets. The reactions at a fixed
357 temperature were carried out using a magnetic stirrer with a contact thermometer Heidolph MR
358 2001.

359 4.1.1. General procedure for the synthesis of selenocyanates

360 Selenocyanates were synthesized using the general protocol described by Wheeler and
361 Merriam with some modifications [28]. According to this procedure, alkyl halides (10-20 mmol)
362 were treated with KSeCN (12-25 mmols) of in ethanol (10- 20 ml). The reaction mixture was refluxed
363 for 6 h and the progress of the reaction was monitored periodically by Thin Layer Chromatography
364 (TLC). After the completion of the reaction, the inorganic salt was separated by filtration and the
365 filtrate was purified with charcoal, condensed and crystallized with ethanol, to yield crystals of
366 arylmethylselenocyantes (**1**-**13**). Synthesis and chemical characteristics of compounds **1**, **3**-**7** and
367 **10**-**12** have been described in the literature [47-49]. Analytical data for the compounds (**1**, **3**-**7** and
368 **10**-**12**) are in agreement with the values reported in the literature (see Supplementary).

369 4.1.1.1. 4-Methylbenzyl selenocyanate (**2**)

370 4-Methylbenzyl chloride (1.4g, 10 mmol), KSeCN (1.73g, 12mmol) and ethanol (10 ml) were
371 used. The compound **2** was obtained as light crystals. Yield 83.6% (1,76g, 8.36 mmol); TLC R*f* (DCM,
372 100%): 0.51. ^{1}H NMR (DMSO-d6, ppm): δ 7.23 (d, *J*= 7.62 Hz, 2H, 2 C-H), 7.17 (d, *J*=8.21 Hz, 2H, 2
373 C-H), 4.27 (s, 2H, CH_2), 2.28 (t, *J*=9.10 Hz, 3H, CH_3). ^{13}C NMR (DMSO-d6, ppm): δ 137.62,135.65,
374 129.61,129.22,105.39 (Se-CN), 33.08, 21.22. LC–MS: purity 100 %, t_R = 6.25, (ESI) m/z: calculated for
375 C_9H_9NSe $[M+H]^+$: 105.07, found: 105.02.

376 4.1.1.2. 3-Chlorobenzyl selenocyanate (**8**)

377 3-Chlorobenzyl chloride (3.22g, 20 mmol), KSeCN (3.60g. 25 mmol) and ethanol (20 ml) were
378 used. The compound **8** was obtained as light crystals. Yield 82.55 % (3.81g, 16.51 mmol); TLC R*f*
379 (DCM, 100%): 0.75. ^{1}H NMR (DMSO-d6, ppm): δ 7.42(m, 1H, CH), 7.37 (m, 2H, CH), 7.33 (m, 1H,
380 CH), 4.28 (t, *J*=9.15 Hz, 2H, CH_2). ^{13}C NMR (DMSO-d6, ppm): δ 141.45, 133.38, 130.95, 129.04, 128.17,
381 128.00, 105.23(Se-CN), 31.96. LC–MS: purity 98.95 %, t_R = 6.24, (ESI) m/z: calculated for C_8H_6ClNSe
382 $[M+H]^+$: 125.02, found: 125.02.

 doi:10.20944/preprints201802.0142.v1

4.1.1.3. 3,4-Dichlorobenzyl selenocyanate (**9**)

3,4-Dichlorobenzyl chloride (3.91g, 20 mmol), KSeCN (3.6g. 25 mmol) and ethanol (20 ml) were used. The compound **9** was obtained as yellow crystals. Yield 88.2 % (4.673g, 17.64 mmol); TLC R*f* (DCM, 100%): 0.60. ^{1}H NMR (DMSO-d6, ppm): δ 7.62(m, 2H, CH), 7.37(dd, J_1=2.12 Hz, J_2=2.09 Hz, 1H, CH), 4.28 (t, *J*=9.15 Hz, 2H, CH_2). ^{13}C NMR (DMSO-d6, ppm): δ 140.24, 131.29 (4 C), 129.67, 105.19 (Se-CN), 31.23. LC–MS: purity 99.49 %, t_R = 6.86, (ESI) m/z: calculated for $C_8H_5Cl_2NSe$ $[M+H]^+$: 158.98, found: 158.97.

4.1.1.4. 1-(Selenocyanatomethyl)naphthalene (**13**)

1- Chloromethyl naphthalene (3.533g, 20 mmol), KSeCN (3.6g. 25 mmol) and ethanol (20 ml) were used. The compound **13** was obtained as yellow crystals. Yield 75.5 % (3.71g, 15.1 mmol); TLC R*f* (DCM, 100%): 0.64. ^{1}H NMR (DMSO-d6, ppm): δ 8.27 (d, *J*=8.21 Hz, 1H, CH), 7.96 (dd, J_1=7.03 Hz, J_2= 7.03 Hz, 2H, CH), 7.49 (m, 4H, CH), 4.78 (t, *J*=9.38 Hz, 2H, CH_2). ^{13}C NMR (DMSO-d6, ppm): δ 134.0^2, 130.87, 129.21, 128.61, 126.77, 125.73, 124.54, 105.33 (Se-CN), 31.09. LC–MS: purity 94.69%, t_R = 6.59, (ESI) m/z: calculated for $C_{12}H_9NSe$ $[M+H]^+$: 141.07, found: 141.03.

4.2. X-ray crystallography

Single crystals suitable for X-ray analysis were obtained from ethanol for **1** and butan-2-ol for **12** by slow evaporation of the solvent at room temperature. Intensity data of **1** was collected on the Bruker-Nonius Kappa CCD four circle diffractometer, whereas of **12** was collected on Oxford Diffraction SuperNova Diffractometer equipped with a Mo (0.71069 Å) Kα radiation source. Position of non-hydrogen atoms were determined by direct method using SIR-2014 program [50]. Hydrogen atoms bonded to carbons atoms were included at idealized positions and were refined using a riding model. The aryl hydrogen atoms were constrained with C-H 0.93 Å, the methylene groups with C-H 0.97 Å and $U_{iso}(H) = 1.2U_{eq}$. The final refinements were performed by SHELXL program [51], ORTEP [52] and MERCURY [53] programs were employed for molecular graphics.

Compound 1: C_8H_7NSe, Mr = 196.11, crystal size 0.08 x 0.16 x 0.46 mm^3, monoclinic, space group $P2_1/c$, a = 5.9880(1) Å, b = 7.4440(2) Å, c = 17.4880(5) Å, β = 96.277(2)°, V = 774.85 Å^3, Z = 4, T = 100(2)K, 6844 reflections collected, 1786 unique reflections [R_{INT} = 0.0326], R1 = 0.0226, wR2 = 0.0521 [I > 2σ(I)], R1 = 0.0226, wR2 = 0.0536 [all data].

Compound 12: $C_{12}H_9NSe$, Mr = 246.16, crystal size 0.25 x 0.48 x0.60 mm^3, monoclinic, space group Ia, a = 8.2486(2) Å, b = 5.9838(1) Å, c = 20.4158(7) Å, β = 93.097(3)°, V = 1006.23 Å^3, Z = 4, T = 130(2)K, 4415 reflections collected, 2048 unique reflections [R_{INT} = 0.0300], R1 = 0.0368, wR2 = 0.0921 [I > 2σ(I)], R1 = 0.0397, wR2 = 0.0947 [all data].

CCDC 1819893-1819894 contain the supplementary crystallographic data for this manuscript. The data can be obtained free of charge from The Cambridge Crystallographic Data Centre via www.ccdc.cam.ac.uk/data_request/cif.

4.3. Antimicrobial activity

4.3.1.Antimicrobial susceptibility testing

The minimal inhibitory concentration tests were performed by the standard microdilution method in cation-adjusted Mueller-Hinton II Broth (MHB, Becton-Dickinson, Germany) according to

 doi:10.20944/preprints201802.0142.v1

Clinical and Laboratory Standard Institute (CLSI) recommendations [54]. The compounds (**1**-**13**) were evaluated for their antimicrobial activity against a broad spectrum of microorganisms, including Gram-positive bacteria (*S. carnosus* and *S. aureus),* Gram-negative bacteria (*A. baumanni* and *P. aeruginosa*) and yeasts (*C. albicans* and *S. cerevisiae*). The values of MIC were recorded after incubation of compounds for 20 h and 24 h with bacteria and yeast, respectively. The experiments were performed in triplicate and on three different occasions (*i.e.* a total of nine times).

4.3.2. Nematicidal activity

The compounds were also evaluated for their nematicidal activity against model nematode (*Steinernema feltiae*). *S. feltiae* was obtained from Sautter and Stepper GmbH (Ammerbuch, Germany). The assay was performed according to the protocol mentioned in the literature [55,56]. Results are represented as means ± SD. GraphPad Prism 5 was used to perform the statistical analysis. Statistical significances were calculated by employing GraphPad Prism 5 and calculations were performed using one-way ANOVA, with $p < 0.05$ considered to be statistically significant.

4.4. Cytotoxic activity

4.4.1. Cell lines

L5178 mouse T-cell lymphoma cells (PAR) (ECACC Cat. No. 87111908, obtained from FDA, Silver Spring, MD, USA) were transfected with pHa MDR1/A retrovirus, as previously described by Cornwell *et al.* [57]. The ABCB1-expressing cell line L5178Y (MDR) was selected by culturing the infected cells with colchicine. The parental L5178 mouse T-cell lymphoma cells and the L5178Y human ABCB1-transfected subline was cultured in McCoy's 5A medium (Sigma-Aldrich, St Louis, MO, USA) supplemented with 10% heat-inactivated horse serum (Sigma-Aldrich, St Louis, MO, USA), 200 mM L-glutamine (Sigma-Aldrich, St Louis, MO, USA) and a penicillin-streptomycin (Sigma-Aldrich, St Louis, MO, USA) mixture in concentrations of 100 U/L and 10 mg/L, respectively. The cell lines were incubated at 37°C, in a 5% CO_2, 95% air atmosphere.

NIH/3T3 mouse embryonic fibroblast cell line (ATCC CRL-1658) was purchased from LGC Promochem, Teddington, UK. The cell line was cultured in Dulbecco's Modified Eagle's Medium (DMEM, containing 4.5g/L glucose) supplemented with 10% heat-inactivated fetal bovine serum. The cell line was incubated at 37°C, in a 5% CO_2, 95% air atmosphere.

4.4.2. Assay for cytotoxic effect

Cytotoxicity assays were performed following the procedure described in the literature [58,59]. Parental and multidrug resistant mouse T-lymphoma cells and NIH/3T3 non-cancerous mouse embryonic fibroblast cell lines were used to determine the effect of the selenocyanates on the growth of cells. The effects of increasing concentrations of selenocyanates on cell growth were tested in 96-well flat-bottomed microtiter plates. The compounds were diluted in a volume of 100 µL of medium.

The adherent mouse embryonic fibroblast cells were cultured in 96-well flat-bottomed microtiter plates, using DMEM supplemented with 10% heat-inactivated fetal bovine serum. The culture plates were incubated at 37°C, in a 5% CO_2, 95% air atmosphere. In a separate plate, the respective dilutions of the selenocyanates were prepared. The density of the cells was adjusted to

Preprints (www.preprints.org) | NOT PEER-REVIEWED | Posted: 22 February 2018 doi:10.20944/preprints201802.0142.v1

$1x10^4$ cells per well, the cells were seeded for 4 h at 37°C, 5% CO_2, then the medium was removed from the plates containing the cells, and the dilutions previously made were added to the cells.

In case of the mouse T-lymphoma cells, the two-fold serial dilutions were prepared in 100 µL of McCoy's 5A, horizontally. The parental (PAR) and multi-drug resistant (MDR) mouse T-lymphoma cells were adjusted to a density of 1×10^4 cells in 100 µL of McCoy's 5A medium and were added to each well, with the exception of the medium control wells.

The culture plates were incubated at 37°C for 24 h; at the end of the incubation period, 20 µL of MTT (thiazolyl blue tetrazolium bromide, Sigma) solution (from a stock solution of 5 mg/ml) were added to each well. After incubation at 37°C for 4 h, 100 µL of sodium dodecyl sulfate (SDS) (Sigma) solution (10% in 0.01 M HCI) were added to each well and the plates were further incubated at 37°C overnight. Cell growth was determined by measuring the optical density (OD) at 540/630 nm with Multiscan EX ELISA reader (Thermo Labsystems, Cheshire, WA, USA). Inhibition of the cell growth was determined according to the formula below:

$$IC_{50} = 100 - \left[\frac{OD\ sample - OD\ medium\ control}{OD\ cell\ control - OD\ medium\ control}\right] \times 100$$

Results have been expressed in terms of IC_{50}, defined as the inhibitory dose that reduces the growth of the cells exposed to the tested compounds by 50%, each representing the mean of a minimum of three independent experiments.

4.5. Evaluation of rhodamine 123 (R123) retention by flow cytometry

The potency of the tested compounds as inhibitors of the ABCB1 efflux pump was determined using a fluorescence-based detection system, described previously in the literature [38,59]. Verapamil was applied as a reference inhibitor of the ABCB1 transporter. The parental (PAR) and multidrug resistant (MDR) mouse T-lymphoma cells were adjusted to a density of 2×10^6/ml, re-suspended in serum-free McCoy's 5A medium and distributed in 0.5 ml aliquots into Eppendorf centrifuge tubes. The tested compounds (1 and 10 µl, from a stock solution of 1mM) were added at different concentrations (2 µM and 20 µM final concentrations, respectively), and the samples were incubated for 10 min at room temperature. Subsequently, 10 µl (with a final concentration of 5.2 µM) of rhodamine 123 was added to the samples and the cells were incubated for 20 minutes at 37°C, washed twice and re-suspended in 0.5 ml phosphate buffered saline (PBS) for analysis. The fluorescence intensity of the cell population was measured with a Partec CyFlow flow cytometer (Partec, Munster, Germany). Verapamil was used as a positive control at 20 µM final concentration in the rhodamine 123 exclusion experiments. The mean fluorescence intensity (%) was calculated for the treated MDR and PAR mouse T-lymphoma cells as compared to the untreated cells. The fluorescence activity ratio (FAR) was calculated based on the following equation which relates the measured fluorescence values:

$$FAR = \frac{MDR_{treated}/MDR_{control}}{parental_{treated}/parental_{control}}\ ;\ Quotient = 100\ x\ (FAR_{compound}/FAR_{verapamil})$$

4.6. Mutagenicity assay

4.6.1. Reagents for microplate fluctuation Ames test

4-nitroquinoline-N-oxide (NQNO), DMSO, ebselen, bromocresol purple, $NADP^+$, glucose-6-phosphate sodium salt and glucose-6-phosphate dehydrogenase were purchased from

 doi:10.20944/preprints201802.0142.v1

Sigma-Aldrich (Seelze, Germany); ampicillin was obtained from Polfa Tarchomin S.A. (Warszawa, Poland); beef extract, L-histidine monochloride, D-biotin,; peptone from casein, water for HPLC analysis from Merck (Darmstadt, Germany); potassium phosphate monobasic, potassium phosphate, ammonium sulfate, trisodium citrate dehydrate, magnesium sulfate heptahydrate, sodium chloride, potassium chloride, sodium phosphate dibasic, D-glucose from Chempur (Piekary Śląskie, Poland).

4.6.2. Bacterial strains in the mutagenicity assay

The *Salmonella typhimurium* TA100 strain with base pair substitution (*hisG46* mutation, which target is GGG) was purchased from Xenometrix, Allschwil, Switzerland, and has been used in Ames 384 - well microtiter assay [60].

4.6.3. Modified Ames 384 - well microtiter assay

Prior to the experiment, *Salmonella typhimurium* TA100 strain was cultivated overnight (NB-2 liquid medium in the presence of 25 μg/ml ampicillin). Then, all of the tested compounds were assayed according to microtiter liquid Ames fluctuation protocol described in the literature [60]. NQNO was used as a positive control in the mutagenicity assays. This reagent causes point mutations in the genome as it induces G:C →A:T transitions in the *Salmonella typhimurium* TA-100 strain [60].

4.7. In vitro PAMPA permeability assay

4.7.1. Reagents

Pre-coated PAMPA Plate System Gentest™ was purchased from Corning (Bradford, MA, USA). Boric acid (0.4 M) and 0.1 M sodium borate decahydrate (both HPCE grade, in the water) were obtained from Beckman Coulter (USA). Sodium hydroxide and hydrochloric acid for CE were purchased from Fluka - Sigma Aldrich (Seelze, Germany). Water for HPLC analysis was purchased from Merck (Darmstadt, Germany). Potassium phosphate monobasic, sodium phosphate dibasic, sodium chloride and potassium chloride were obtained from Chempur (Piekary Śląskie, Poland). Reference compounds: caffeine and norfloxacin were purchased from Sigma-Aldrich (St. Louis, MO, USA).

4.7.2. Methods of permeability measurement

The tested compounds (**1**, **2**, **4**, and **13**) and reference probes were prepared in PBS buffer (pH = 7.4) from 10 mM DMSO stocks, according to previously described protocol [40]. The concentrations, both the tested compounds and references (caffeine, and norfloxacin) were estimated in the donor and acceptor compartments, using the capillary electrophoresis technique (CE). Moreover, the calibration curves of all above mentioned test and reference compounds were determined by the same technique. Finally, the permeability coefficients (Pe, [cm/s]) of the test compounds were calculated using the formula provided by the PAMPA Plate System manufacturer [40,42].

4.8. Analytical methods- Ames and in vitro PAMPA methods

 doi:10.20944/preprints201802.0142.v1

The results of the modified Ames microtiter test were additionally read at 420 nm, using microplate reader (Perkin Elmer, EnSpire). In the PAMPA experiments, the concentrations of the tested compounds were determined using capillary electrophoresis (CE) system P/ACE MDQ (Beckman Coulter, Fullerton, CA, USA), controlled by 32 Karat Software version 8.0. The CE system was equipped with diode-array detector (DAD) and analytical uncoated fused-silica capillary with total length of 60 cm (50.2 cm to detection window) and internal diameter 75 μm,) purchased from Beckman.

Acknowledgments: Authors acknowledge the financial support provided by the Jagiellonian University, Krakow, Poland (project K/ZDS/005593), University of Saarland, Saarbruecken, Germany and INTERREGVAGR program (BIOVAL, Grant No. 4-09-21). We also acknowledge the support of Erasmus + mobility programme 2016-2017. Special thanks go to many other colleagues from the Academics International network (www.academiacs.eu) for their helpful discussions and advice. Gabriella Spengler was supported by the János Bolyai Research Scholarship of the Hungarian Academy of Sciences. Annamária Kincses and Márió Gajdács were supported by the UNKP-17-3 New National Excellence Program of the Ministry of Human Capacities.

Author Contributions: M.J.N., K.W., G.S., J.H. and C.J. conceived and designed the experiments; M.J.N. synthesized the compounds; E.Ż. and W.N. performed crystallographic studies; K.W., M.J.N. and M.S. performed the experiments with microbes; A.K., M.G. and G.S. performed the experiments with mammalian cells; M.A.M. and M.J.N. performed ADMET studies *in vitro*; G.L. and K.K.-K. supervised ADMET studies *in vitro;* E.K. supervised microbiological studies; M.J.N., K.W., C.J. and J.H. wrote the paper.

Conflicts of Interest: The authors declare no conflict of interest.

References

[1] Davies, J.; Davies, D. Origins and evolution of antibiotic resistance. *Microbiol. Mol. Biol. Rev.* **2010**, *74*, 417-433.

[2] Moloney, M.G. Natural products as a source for novel antibiotics. *Trends Pharmacol. Sci.* **2016**, *37*, 689-701.

[3] Brown, D.G.; Lister ,T.; May-Dracka, T.L. New natural products as new leads for antibacterial drug discovery. *Bioorg. Med. Chem. Lett.* **2014**, *24*, 413-418.

[4] Wencewicz, T.A. New antibiotics from nature's chemical inventory. *Bioorgan. Med. Chem.* **2016**, *24*, 6227-6252.

[5] Adetumbi, M.A.; Lau, B.H.S. *Allium-Sativum* (garlic) - a natural antibiotic. *Med. Hypotheses* **1983**, *12*, 227-237.

[6] Reyes-Jurado, F.; Lopez-Malo, A.; Palou, E. Antimicrobial activity of individual and combined essential oils against foodborne pathogenic bacteria. *J. Food Protect.* **2016**, *79*, 309-315.

[7] Subramani, R.; Narayanasamy, M.; Feussner, K.D. Plant-derived antimicrobials to fight against multi-drug-resistant human pathogens. *3 Biotech.* **2017**, *7*, 172.

[8] Cushnie, T.P.; Cushnie, B.; Lamb, A.J. Alkaloids: an overview of their antibacterial, antibiotic-enhancing and antivirulence activities. *Int. J. Antimicrob. Ag.* **2014**, *44*, 377-386.

[9] Cushnie, T.P.; Lamb, A.J. Antimicrobial activity of flavonoids. *Int. J. Antimicrob. Agents.* **2005**, *26*, 343-356.

[10] Toure, D.; Kouame, P.; Bedi, G.; Djaman, A.J.; Guesssennd, N.; Oussou, R.; Dinzedi, R.; Chalchat, J.C.; Dosso, M.; Tonzibo, F. Terpenes, antibacterial and modulatory antibiotic activity of essential oils from *Croton hirtus* L' Her. (*Euphorbiaceae*) from Ivory Coast. *J. Essent. Oil Bear. Pl.* **2014**, *17*, 607-616.

[11] Coppo, E.; Marchese, A. Antibacterial activity of polyphenols. *Curr. Pharm. Biotechnol.* **2014**, *15*, 380-390.

[12] Reiter, J.; Levina, N.; van der Linden, M.; Martin, C.; Slusarenko, A.J. Diallylthiosulfinate (allicin), a volatile antimicrobial from garlic (*Allium sativum*), kills human lung pathogenic bacteria, including MDR strains, as a vapor. *Molecules* **2017**, *22*, 1-14.

[13] Kalaras, M.D.; Richie, J.P.; Calcagnotto, A.; Beelman, R.B. Mushrooms: a rich source of the antioxidants ergothioneine and glutathione. *Food Chem.* **2017**, *233*, 429-433.

[14] Ko, M.O.; Kim, M.B.; Lim, S.B. Relationship between chemical structure and antimicrobial activities of isothiocyanates from cruciferous vegetables against oral pathogens. *J. Microbiol. Biotechn.* **2016**, *26*, 2036-2042.

[15] Dufour, V.; Stahl, M.; Baysse, C. The antibacterial properties of isothiocyanates. *Microbiology* **2015**, *161*, 229-243.

[16] Thomas, E.L.; Aune, T.M. Lactoperoxidase, peroxide, thiocyanate antimicrobial system: correlation of sulfhydryl oxidation with antimicrobial action. *Infection and immunity* **1978**, *20*, 456-463.

[17] Oram, J.D.; Reiter, B. The inhibition of Streptococci by lactoperoxidase, thiocyanate and hydrogen peroxide. The oxidation of thiocyanate and the nature of the inhibitory compound. *Biochem. J.* **1966**, *100*, 382-388.

[18] Collins, R.; Johansson, A.L.; Karlberg, T.; Markova, N.; van den Berg, S.; Olesen, K.; Hammarström, M.; Flores, A.; Schüler, H.; Schiavone, L.H.; Brzezinski, P.; Arnér, E.S.; Högbom, M. Biochemical discrimination between selenium and sulfur 1: a single residue provides selenium specificity to human selenocysteine lyase. *Plos One* **2012**, *7*, e30581.

[19] Yarema, M.C.; Curry, S.C. Acute tellurium toxicity from ingestion of metal-oxidizing solutions. *Pediatrics* **2005**, *116*, 319-321.

[20] Kil, J.; Lobarinas, E.; Spankovich, C.; Griffiths, S.K.; Antonelli, P.J.; Lynch, E.D.; Le Prell, C.G. Safety and efficacy of ebselen for the prevention of noise-induced hearing loss: a randomised, double-blind, placebo-controlled, phase 2 trial. *Lancet* **2017**, *390*, 969-979.

[21] Nasim, M.J.; Ali, W.; Domínguez-Álvarez, E.; da Silva Júnior, E.N.; Saleem, R.S.Z.; Jacob, C. Reactive selenium species: redox modulation, antioxidant, antimicrobial and anticancer activities. *Organoselenium Compounds in Biology and Medicine: Synthesis, Biological and Therapeutic Treatments.* The Royal Society of Chemistry **2018**, 277-302.

[22] Du, P.; Viswanathan, U.M.; Xu, Z.J.; Ebrahimnejad, H.; Hanf, B.; Burkholz, T.; Schneider, M.; Bernhardt, I.; Kirsch, G.; Jacob, C. Synthesis of amphiphilic seleninic acid derivatives with considerable activity against cellular membranes and certain pathogenic microbes. *J. Hazard. Mater.* **2014**, *269*, 74-82.

[23] Salama, P.; Bernard, C. Chemoselective synthesis of functionalized diselenides. *Tetrahedron Lett.* **1995**, *36*, 5711-5714.

[24] Baquedano, Y.; Alcolea, V.; Toro, M.A.; Gutiérrez, K.J.; Nguewa, P.; Font, M.; Moreno, E.; Espuelas, S.; Jiménez-Ruiz, A.; Palop, J.A.; Plano, D.; Sanmartín, C. Novel heteroaryl selenocyanates and diselenides as potent antileishmanial agents. *Antimicrob. Agents Chemother.* **2016**, *60*, 3802-3812.

[25] Żesławska, E.; Korona-Głowniak, I.; Szczesio, M.; Olczak, A.; Żylewska, A.; Tejchman, W.; Malm, A. Structural analysis and antimicrobial activity of 2[1H]-pyrimidinethione/selenone derivatives. *J. Mol. Struct.* **2017**, *1142*, 261-266.

[26] Estevam, E.C.; Witek, K.; Faulstich, L.; Nasim, M.J.; Latacz, G.; Domínguez-Álvarez, E.; Kieć-Kononowicz, K.; Demasi, M.; Handzlik, J.; Jacob, C. Aspects of a distinct cytotoxicity of selenium salts and organic selenides in living cells with possible implications for drug design. *Molecules* **2015**, *20*, 13894-13912.

[27] Witek, K.; Nasim, M.J.; Bischoff, M.; Gaupp, R.; Arsenyan, P.; Vasiljeva, J.; Marć, M.A.; Olejarz, A.; Latacz, G.; Kieć-Kononowicz, K.; Handzlik, J.; Jacob, C. Selenazolinium salts as "small molecule catalysts" with high potency against ESKAPE bacterial pathogens. *Molecules* **2017**, *22*, 1-16.

[28] Wheeler, H.L.; Merriam, H.F. On the action of alkyl thiocyanates and alkyl isothiocyanates with thiol acids. *J. Am. Chem. Soc.* **1901**, *23*, 283-299.

[29] Żesławska, E.; Oleksyn, B.J.; Korohoda, M.J.; Śliwiński, J. The crystal and molecular structure of 1-methyl-4-(p-methylbenzylidene)-2-methylseleno-5-imidazolinone. *Pol. J. Chem.* **2000**, *74*, 751-757.

[30] Maartmannmoe, K.; Sanderud, K.A.; Songstad, J. The crystal structure of 4-nitrobenzyl tellurocyanate, 4-nitrobenzyl selenocyanate, 4-nitrobenzyl thiocyanate and benzyl selenocyanate. *Acta Chem. Scand.* **1984**, *38*, 187-200.

[31] Groom, C.R.; Bruno, I.J.; Lightfoot, M.P.; Ward, S.C. The Cambridge structural database. *Acta Crystallogr. B Struct. Sci. Cryst. Eng. Mater.* **2016**, *72*, 171-179.

[32] Nunes, R.S.C.; Del Aguila, E.; Paschoalin, V.M.F. Safety evaluation of the coagulase-negative Staphylococci microbiota of salami: superantigenic toxin production and antimicrobial resistance. *Biomed. Res. Int.* **2015**, *2015*, 1-17.

[33] Li, J.; Nation, R.L.; Owen, R.J.; Wong, S.; Spelman, D.; Franklin, C. Antibiograms of multidrug-resistant clinical *Acinetobacter baumannii*: Promising therapeutic options for treatment of infection with colistin-resistant strains. *Clin. Infect. Dis.* **2007**, *45*, 594-598.

[34] Tamma, P.D.; Turnbull, A.E.; Milstone, A.M.; Hsu, A.J.; Carroll, K.C.; Cosgrove, S.E Does the piperacillin minimum inhibitory concentration for *Pseudomonas aeruginosa* influence clinical outcomes of children with pseudomonal bacteremia? *Clin. Infect. Dis.* **2012**, *55*, 799-806.

[35] Nenoff, P.; Oswald, U.; Haustein, U.F. *In vitro* susceptibility of yeasts for fluconazole and itraconazole. Evaluation of a microdilution test. *Mycoses* **1999**, 42, 629-639.

[36] Kronvall, G.; Karlsson, I. Fluconazole and voriconazole multidisk testing of *Candida* species for disk test calibration and MIC estimation. *J. Clin. Microbiol.* **2001**, *39*, 1422-1428.

[37] Żesławska, E.; Kincses, A.; Spengler, G.; Nitek, W.; Wyrzuc, K.; Kieć-Kononowicz, K.; Handzlik, J. The 5-aromatic hydantoin-3-acetate derivatives as inhibitors of the tumour multidrug resistance efflux pump P-glycoprotein (ABCB1): synthesis, crystallographic and biological studies. *Bioorgan. Med. Chem.* **2016**, *24*, 2815-2822.

[38] Domínguez-Álvarez, E.; Gajdács, M.; Spengler, G.; Palop, J.A.; Marć, M.A.; Kieć-Kononowicz, K.; Amaral, L.; Molnár, J.; Jacob, C.; Handzlik, J.; Sanmartín, C. Identification of selenocompounds with promising properties to reverse cancer multidrug resistance. *Bioorg. Med. Chem. Lett.* **2016**, *26*, 2821-2824.

[39] Marć, M.A.; Domínguez-Álvarez, E.; Słoczyńska, K.; Żmudzki, P.; Chłoń-Rzepa, G.; Pękala, E. *In vitro* biotransformation, safety, and chemopreventive action of novel 8-methoxy-purine-2,6-dione derivatives. *Appl. Biochem. Biotech.* **2018**, *184*, 124-139.

[40] Latacz, G.; Lubelska, A.; Jastrzębska-Więsek, M.; Partyka, A.; Sobiło, A.; Olejarz, A.; Kucwaj-Brysz, K.; Satała, G.; Bojarski, A.J.; Wesołowska, A.; Kieć-Kononowicz, K.; Handzlik, J. In the search for a lead structure among series of potent and selective hydantoin 5-HT$_7$R agents: the drug-likeness *in vitro* study. *Chem. Biol. Drug Des.* **2017**, *90*, 1295-1306.

[41] Yu, H.; Wang, Q.; Sun, Y.; Shen, M.; Li, H.; Duan, Y. A new PAMPA model proposed on the basis of a synthetic phospholipid membrane. *Plos One* **2015**, *10*, e0116502.

[42] Chen, X.X.; Murawski, A.; Patel, K.; Crespi, C.L.; Balimane, P.V. A novel design of artificial membrane for improving the PAMPA model. *Pharm. Res.* **2008**, *25*, 1511-1520.

[43] Mahmood, H.Y.; Jamshidi, S.; Sutton, J.M.; Rahman, K.M. Current advances in developing inhibitors of bacterial multidrug efflux pumps. *Curr. Med. Chem.* **2016**, *23*, 1062-1081.

[44] Jacob, C. Redox signalling via the cellular thiolstat. *Biochem. Soc. Trans.* **2011**, *39*, 1247-1253.

[45] Domínguez-Álvarez, E.; Plano, D.; Font, M.; Calvo, A.; Prior, C.; Jacob, C.; Palop, J.A.; Sanmartín, C. Synthesis and antiproliferative activity of novel selenoester derivatives. *Eur. J. Med. Chem.* **2014**, *73*, 153-166.

[46] Gajdács, M.; Spengler, G.; Sanmartín, C.; Marć, M.A.; Handzlik, J.; Domínguez-Álvarez, E. Selenoesters and selenoanhydrides as novel multidrug resistance reversing agents: a confirmation study in a colon cancer MDR cell line. *Bioorg. Med. Chem. Lett.* **2017**, *27*, 797-802.

[47] Plano, D.; Baquedano, Y.; Moreno-Mateos, D.; Font, M.; Jiménez-Ruiz, A.; Palop, J.A.; Sanmartín, C. Selenocyanates and diselenides: a new class of potent antileishmanial agents. *Eur. J. Med. Chem.* **2011**, *46*, 3315-3323.

[48] Suzuki, H.; Usuki, M.; Hanafusa, T. A photochemical route to some substituted benzyl isoselenocyanates. *Synthesis* **1979**, *1979*, 705-707.

[49] Jacob, L.A.; Matos, B.; Mostafa, C.; Rodriguez, J.; Tillotson, J.K. A facile synthesis of substituted benzyl selenocyanates. *Molecules* **2004**, *9*, 622-626.

[50] Burla, M.C.; Caliandro, R.; Carrozzini, B.; Cascarano, G.L.; Cuocci, C.; Giacovazzo, C.; Mallamo, M.; Mazzone, A.; Polidori, G. Crystal structure determination and refinement via SIR2014. *J. Appl. Crystallogr.* **2015**, *48*, 306-309.

[51] Sheldrick, G.M. Crystal structure refinement with SHELXL. *Acta Crystallogr. C Struct. Chem.* **2015**, *71*, 3-8.

[52] Farrugia, L.J. WinGX and ORTEP for Windows: an update. *J. Appl. Crystallogr.* **2012**, *45*, 849-854.

[53] Macrae, C.F.; Edgington, P.R.; McCabe, P.; Pidcock, E.; Shields, G.P.; Taylor, R.; Towler, M.; van de Streek, J. Mercury: visualization and analysis of crystal structures. *J. Appl. Crystallogr.* **2006**, *39*, 453-457.

[54] Clinical and Laboratory Standards Institute. *Document M07-A9 Methods for Dilution Antimicrobial Susceptibility Tests for Bacteria that Grow Aerobically, Approved Standard*, 9th ed.; Clinical and Laboratory Standards Institute: Wayne, PA, USA, 2012.

[55] Schneider, T.; Baldauf, A.; Ba, L.A.; Jamier, V.; Khairan, K.; Sarakbi, M.B.; Reum, N.; Schneider, M.; Röseler, A.; Becker, K.; Burkholz, T.; Winyard, P.G.; Kelkel, M.; Diederich, M.; Jacob C. Selective antimicrobial activity associated with sulfur nanoparticles. *J. Biomed. Nanotechnol.* **2011**, **7**, 395-405.

[56] Mániková, D.; Letavayová, L.M.; Vlasáková, D.; Košík, P.; Estevam, E.C.; Nasim, M.J.; Gruhlke, M.; Slusarenko, A.; Burkholz, T.; Jacob, C.; Chovanec, M. Intracellular diagnostics: Hunting for the mode of action of redox-modulating selenium compounds in selected model systems. *Molecules* **2014**, *19*, 12258-12279.

[57] Cornwell, M.M.; Pastan, I.; Gottesman, M.M. Certain calcium-channel blockers bind specifically to multidrug-resistant human KB carcinoma membrane vesicles and inhibit drug binding to P-glycoprotein. *J. Biol. Chem.* **1987**, *262*, 2166-2170.

[58] Takács, D.; Csonka, Á.; Horváth, Á.; Windt, T.; Gajdács, M.; Riedl, Z.; Hajós, G.; Amaral, L.; Molnár, J.; Spengler, G. Reversal of ABCB1-related multidrug resistance of colonic adenocarcinoma cells by phenothiazines. *Anticancer Res.* **2015**, *35*, 3245-3251.

[59] Spengler, G.; Evaristo, M.; Handzlik, J.; Serly, J.; Molnár, J.; Viveiros, M.; Kiéc-Kononowicz, K.; Amaral L. Biological activity of hydantoin derivatives on P-glycoprotein (ABCB1) of mouse lymphoma cells. *Anticancer Res.* **2010**, *30*, 4867-4871.

[60] Zeiger, E. Bacterial mutation assays. *Methods Mol. Biol.* **2013**, *1044*, 3-26.

Sample Availability: Samples of the compounds are not available from the authors.